Published in final edited form as:
Clin Exp Metastasis. 2013 April ; 30(4): 541–552. doi:10.1007/s10585-012-9558-1.

INTEGRIN α3β1 REGULATES TUMOR CELL RESPONSES TO STROMAL CELLS AND CAN FUNCTION TO SUPPRESS PROSTATE CANCER METASTATIC COLONIZATION

Afshin Varzavand[1], **Justin M. Drake**[2], **Robert U. Svensson**[2], **Mary E. Herndon**[1], **Bo Zhou**[1], **Michael D. Henry**[2,3,4], and **Christopher S. Stipp**[1,2,4]

[1]Department of Biology, University of Iowa, Iowa City, Iowa 52242

[2]Department of Molecular Physiology and Biophysics, University of Iowa, Iowa City, Iowa 52242

[3]Department of Pathology, University of Iowa, Iowa City, Iowa 52242

[4]Holden Comprehensive Cancer Center, University of Iowa, Iowa City, Iowa 52242

Abstract

Integrin α3β1 promotes tumor cell adhesion, migration, and invasion on laminin isoforms, and several clinical studies have indicated a correlation between increased tumoral α3β1 integrin expression and tumor progression, metastasis, and poor patient outcomes. However, several other clinical and experimental studies have suggested that α3β1 can possess anti-metastatic activity in certain settings. To help define the range of α3β1 functions in tumor cells in vivo, we used RNAi to silence the α3 integrin subunit in an aggressive, in vivo-passaged subline of PC-3 prostate carcinoma cells. Loss of α3 integrin impaired adhesion and proliferation on the α3β1 integrin ligand, laminin-332 in vitro. Despite these deficits in vitro, the α3-silenced cells were significantly more aggressive in a lung colonization model in vivo, with a substantially increased rate of tumor growth that significantly reduced survival. In contrast, silencing the related α6 integrin subunit delayed metastatic growth in vivo. The increased colonization of α3-silenced tumor cells in vivo was recapitulated in 3D collagen co-cultures with lung fibroblasts or pre-osteoblast-like cells, where α3-silenced cells showed dramatically enhanced growth. The increased response of α3-silenced tumor cells to stromal cells in co-culture could be reproduced by fibroblast-conditioned medium, which contains one or more heparin binding factors that selectively favor the growth of α3-silenced cells. Our new data suggest a scenario in which α3β1 regulates tumor-host interactions within the metastatic tumor microenvironment to limit growth, providing some of the first direct evidence that specific loss of α3 function in tumor cells can have pro-metastatic consequences in vivo.

Keywords

alpha3 integrin; laminin-332; metastasis; tumor-stromal interaction; heparin-binding growth factors

Introduction

Prostate cancer is the most common cancer in men in the U.S., with 241,740 estimated new cases in 2012, and 28,171 estimated deaths [1]. If distant metastasis has occurred, the five

Address correspondence to: Christopher Stipp, 210 E. Iowa Avenue, BBE 236, Iowa City, IA 52242. Tel: 319-335-0192. Fax: 319-335-1069; christopher-stipp@uiowa.edu.

year survival rate for prostate cancer drops from near 100% to around 30%. Prostate cancer progression involves changes both in the extracellular matrix (ECM) underlying prostate epithelial cells and in the cellular receptors for ECM ligands [2,3,4,5]. Laminins, which are major constituents of the basement membrane beneath prostate epithelial cells, are heterotrimers composed of one α, one β, and one γ subunit. In prostatic intraepithelial carcinoma in situ (PIN) lesions, the continuous layer of the basement membrane protein, laminin-332 (α3β3γ2; LM-332) becomes discontinuous, and in invasive prostate cancer, LM-332 expression is dramatically downregulated or extinguished [6,7]. The loss of LM-332, which plays a crucial role in the maintenance of stable epithelial morphology, may be one of the key events that enable the dissemination of prostate tumor cells.

In contrast to the expression of LM-332, two major laminin receptors, α3 and α6 integrins, are frequently maintained in prostate carcinoma [8]. Integrins, the major family of receptors for ECM ligands, are heterodimers containing one α and one β subunit. The α3 subunit pairs with the β1 subunit to form α3β1 integrin, which binds strongly to LM-332, and to laminin-511 (α5β1γ1; LM-511) [9]. The α6 integrin subunit preferentially pairs with the β4 subunit to form α6β4, a second major receptor for LM-332. In epithelial cells, α6β4 mediates stable anchorage on LM-332 at hemidesmosomes [10]. In contrast, the α3β1 integrin mediates rapid spreading and migration on LM-332 [11,12,13,14], but may also contribute to the formation or maintenance of stable epithelia [15,16,17,18].

In the absence of the β4 subunit, α6 integrin pairs with the β1 subunit instead, and α6β1 integrin binds to a wider array of laminin isoforms, including LM-511 [9]. Like LM-332, the β4 integrin subunit is frequently downregulated during prostate cancer progression, as are other constituents of hemidesmosomes, such as collagen VII and BP180 [6,19,20,21]. In addition, TEM4-18 cells, an aggressive PC-3 prostate carcinoma sub-line selected for enhanced transendothelial migration, were found to have undergone an epithelial-to-mesenchymal transition through upregulation of the transcription factor, ZEB1 [22], which coordinately represses both β4 integrin and LM-332 expression in TEM4-18 cells [23]. Thus, the general view that emerges is that during progression from PIN lesions to invasive prostate cancer, LM-332 and α6β4 integrin are often lost or reduced; however, malignant cells often retain the capacity to interact with LM-332 and other laminin isoforms through the sustained expression of α3β1 or α6β1 integrins.

Sustained expression of α3 and α6 integrin might provide a growth or survival advantage to prostate carcinoma cells by enabling them to bind to LM-511, which, unlike LM-332, is retained in prostate cancer [24]. For example, androgen receptor expression upregulates α6 integrin, which protects laminin-adherent tumor cells from cell death that would otherwise occur upon PI3K inhibition [25]. LM-511 is also abundant in the perineurium of the nerves that innervate the prostate gland, a route of extraprostatic escape for invasive prostate carcinoma cells [5], in endothelial cell basement membranes [26], and in bone marrow stroma [27,28]. Regulated cleavage of the α6 integrin ectodomain, an event that promotes migration and invasion on laminin isoforms [29], has been implicated in bone colonization and in invasion and degradation of bone matrix by metastatic prostate carcinoma cells [30,31]. In contrast to its effect on α6 integrin, de novo androgen receptor expression can reduce (although not extinguish) α3 integrin expression [25], and reduced α3 expression can correlate with a more metastatic phenotype in prostate tumor cells [32]. However, the relationship between α3 expression and prostate cancer progression is complex [8], and the literature is divided in general on the role of α3β1 integrin in metastasis [33,34]. Despite the accumulated evidence that laminin-binding integrins regulate prostate cancer progression, α3 and α6 integrin loss-of-function phenotypes for prostate tumor cells have not yet been described for in vivo assays. Therefore, we created prostate tumor cells with stable, profound, RNAi-mediated silencing of the α3 and α6 integrin subunits. Here we report in

vitro and in vivo studies with these cells that provide evidence that α3 integrin can act as a negative regulator of prostate cancer metastatic colonization and suggest divergent roles for α3 and α6 integrin in regulating prostate cancer progression.

Materials and methods

Antibodies and extracellular matrix proteins

Anti-integrin monoclonal antibodies (mAbs) were anti-α2, A2-IIE10 [34]; anti-α3, A3-X8 [35], and A3-IIF5 [35]; and anti-α6, GoH3 (GeneTex). Rat tail collagen I and growth factor reduced Matrigel were from BD Biosciences. Human laminin-332 (LM-332) was purified from SCC-25 squamous cell carcinoma–conditioned medium as described [13].

Cell culture, RNAi, and retroviral transduction

GS689.Li prostate carcinoma cells [22] and LNCaP C4-2B cells (MD Anderson Cancer Center Characterized Cell Line Core Facility) were cultured in 1:1 high glucose DMEM:F12 with 10% fetal bovine serum (FBS; Valley Biomedical, Inc), 2 mM L-glutamine, 100 U/ml penicillin, 100 ug/ml streptomycin, and 0.1 mM non-essential amino acids (all from Invitrogen). MC3T3-E1 preosteoblastic cells (ATCC) were cultured in MEM alpha medium with 10% fetal bovine serum, 2 mM L-glutamine, 100 U/ml penicillin, and 100 ug/ml streptomycin. Primary human lung fibroblast MRC-5 cells (ATCC) were cultured in high glucose DMEM with 10% fetal bovine serum, 2 mM L-glutamine, 100 U/ml penicillin, and 100 ug/ml streptomycin.

For RNAi, double stranded oligonucleotides encoding short hairpin RNAs (shRNAs) targeting the human α6 and α3 integrin mRNAs were cloned respectively into (i) the original pSIREN RetroQ retroviral vector (BD Biosciences), which contains a puromycin resistance cassette, or (ii) a modified pSIREN vector containing a hygromycin resistance cassette. Two shRNAs targeting different sequences were tested for α3: the α3si targeting sequence is 5’-GGATGACTGTGAGCGGATGAA-3’, and α3si-2 targeting sequence is 5’-TCACTCTGCTGGTGGACTATA-3’. The α6si targeting sequence is 5’-GTATGTAACAGCAACCTTAAA-3’. GS689.Li cells were transduced with these constructs, as previously described [13]. We also transduced cells with a pSIREN hygro vector containing scrambled shRNA control sequence (5’-GTAGTGAAGGATCGTAGACGG-3’), which was based on the α3si targeting sequence and selected not to target any human mRNA known to be expressed. After selecting stably transduced cells, integrin-silenced populations were sorted using a FACS Diva (Becton Dickinson). For doubly silenced cells, α3-silenced GS689.Li cells were transduced with the α6si vector and selected. LNCaP C4-2B cells were transduced with a luciferase cDNA cloned into the pQCXIN retroviral expression vector and selected with G418. These luciferase-expressing C4-2B cells were transduced with an α3 integrin cDNA cloned into the pLXIZ retroviral vector or with the empty pLXIZ vector, and then selected with zeocin. All tumor cell lines were maintained as polyclonal populations. Quantification of dilution series of the GS689.Li cell lines showed that they all had a similar bioluminescences of ~320 photons/sec/cell. The empty vector control and α3 over-expressing LNCaP C4-2B cells both had a bioluminescence of ~50 photons/sec/cell.

Cell surface labeling and immunoprecipitation

GS689.Li cells were labeled on ice for 1 h with 0.1 mg/ml sulfo-NHS-LC-biotin (Thermo-Fisher Pierce) in HBSM (20 mM HEPES PH 7.2, 150 mM Nacl, 5 mM $MgCl_2$). Cells were then rinsed and lysed in 1% Triton X-100 detergent (Sigma-Aldrich) in HBSM containing protease inhibitors (2mM PMSF, 10 ug/ml aprotinin, 5 ug/ml leupeptin and 5 ug/ml E-64; Roche Diagnostics). Specific integrins were immunoprecipitated from clarified lysates, as

previously described [13], and resolved by SDS-PAGE. Proteins were visualized after transfer to nitrocellulose by blotting with IRDye-800-streptavidin (Rockland Immunochemicals, Inc) diluted 1:6500 in Aquablock (East Coast Biologics) with 0.15% Tween-20 (Sigmal-Aldrich). Membranes were scanned with an Odyssey infrared imaging system (LI-COR Biosciences).

Adhesion Assays

Substrates for adhesion assays were 1 ug/ml LM-332, 20 ug/ml collagen I, 100 ug/ml poly-l-lysine (PLL; positive control) or 10 mg/ml heat-inactivated (HI) BSA (negative control). After overnight coating, wells were rinsed and blocked with 10 mg/ml HI BSA. Cells were harvested and resuspended to final concentration of 2×10^5 cells/ml in serum-free medium (SFM) containing 50:50 DMEM:F12, 0.1 mM non-essential amino acids, 25 mM HEPES, 5 mg/ml BSA, and 2 mM L-glutamine. Then 100 ul of cell suspension was added to each of four substrate-coated wells per condition in a 96-well plate. After 25 min at 37°C, 5% CO_2, wells were rinsed three times with warm SFM, with flicking. Positive control PLL wells were gently rinsed once. Cells remaining after rinses were fixed and quantified by staining with crystal violet, as previously described [13]. Adhesion was expressed as fraction of input cells using adhesion in positive control PLL wells to determine total input.

Metastatic Colonization Assays

All animal procedures were performed according to the University of Iowa Animal Care and Use Committee policies. Using a 27-gauge needle, 1×10^6 wild type or integrin-silenced GS689.Li cells were injected into the tail veins of 6-wk-old male *SCID/NCr (BALB/C)* mice (NCI-Frederick) in a volume of 200 μl. Bioluminescent imaging (BLI) was performed in an IVIS100 imaging system (Caliper Life Sciences) after intraperitoneal injection of luciferin (100 μl of 15 mg/ml solution per 10 g) as described previously [36]. Whole body tumor growth rates were measured as follows: a rectangular region of interest was placed around the dorsal and ventral images of each mouse, and total photon flux (photons/sec) was quantified using Living Image software v2.50 (Caliper Life Sciences). The dorsal and ventral values were summed and plotted weekly for each animal. Kaplan–Meier analysis of survival was performed using Prism 4 (GraphPad Software) on the basis that Day 0 was the day of tail vein injections and the end-point was the day of euthanasia as determined by >15% body weight loss, hind limb paralysis or fracture, or by a total photon flux $> 2 \times 10^9$, a value that initial results indicated reliably predicted death within one week in this model.

Cell Spreading Assay

Wild type and α3-silenced cells were plated in SFM on glass-bottomed 35 mm dishes (MatTek Corp) that had been coated with 2 μg/ml LM-332 and blocked with SFM. After 30 min to allow for cell attachment and spreading, cells were photographed with a 20X C Plan phase objective on a Leica DMIRE2 inverted microscope using a Hamamatsu ORCA-285 CCD camera. Cell areas were measured using ImageJ [37].

Proliferation Assays

Wells were coated with 1 μg/ml LM-332, 20 μg/ml collagen I, or left uncoated. A total of 2,500 cells in 200 μl of SFM was plated in 6 wells per cell type per condition in replicate 96 well plates. On subsequent days, replicate plates were developed by discarding 100ul from each well and adding 100 ul of solution containing SFM supplemented with 2% FBS and WST-1 reagent (Roche Diagnostics) diluted 1:10. Plates were incubated for 1 h at 37°C and absorbance at 440 nm was measured using a plate reader.

Matrigel Colony Formation Assay

Wild type and integrin silenced GS689.Li cells (3,000 cells in 35 μl of PC-3 growth medium) were mixed with 350 μl of growth factor reduced Matrigel and plated in the wells of 24 well plates. After Matrigel polymerized for 20 min at 37°C / 5% CO_2, each well was overlaid with 500 μl of either PC-3 growth medium or PC-3 SFM. Plates were incubated for 2–3 weeks before photographing using the inverted microscope system described above.

3D Collagen Assays

Neutralized rat tail collagen solution was prepared at 0.8 mg/ml in DMEM by adding appropriate amounts of 10X DMEM concentrate and 1N NaOH. Next, MRC-5 human lung fibroblasts or MC3T3-E1 murine preosteoblast cells were resuspended at 2.86×10^4 cells/ml in the collagen solution, and 350 μl of cell suspension was plated per well in 24 well plates (for a final cell number of 10,000 stromal cells per well). After 20 min at 37°C, wells containing stromal cells, suspended in polymerized collagen, were overlaid with 3,000 tumor cells per well in 500 μl of SFM. In some experiments, the number of stromal cells per well was varied as indicated. In some experiments, stromal cells were omitted and replaced with serum-free fibroblast conditioned medium at various dilutions. After 3–4 weeks, tumor cell growth was quantified by WST-1 assay or by adding fresh SFM with 0.15 mg/ml luciferin and imaging the plate using the IVIS100 instrument.

Heparin Sepharose Chromatography

A freshly confluent 150 cm^2 flask of MRC-5 fibroblasts was rinsed with PBS and refed with 20 ml of serum-free DMEM containing 5 mg/ml BSA. After 3 days, conditioned medium was collected, centrifuged at 490g for 5 min to remove cell debris, and passed through a 0.45 μm filter. HEPES buffer pH 7.2 was added to a final concentration of 50 mM and 3 ml of starting material was reserved for analysis. The remaining conditioned medium was loaded in 1 ml increments to a 0.4 ml column of Heparin Sepharose 6 Fast Flow (GE Healthcare) pre-equilibrated with PBS. The flow-through fraction was saved and reloaded. The final flow-through fraction was saved, and the column was rinsed with 1 ml steps of 0.15 M, 0.25 M, 0.5 M, 1 M, 1.5 M, and 2 M NaCl in 20 mM HEPES pH 7.2. Next, 50 μl of 20 mg/ml BSA in 20 mM HEPES was added to each fraction and fractions were dialyzed against two changes of PC-3 SFM in Slide-A-Lyzer MINI Dialysis Devices, 3.5K MWCO, (Thermo Fisher Pierce). Samples of each fraction, diluted 1:8 in SFM, were used in 3D collagen growth assays, as described above.

Results

Specific silencing of α3 and α6 integrin in prostate carcinoma cells

To investigate the α3 and α6 integrin loss-of-function phenotypes in a model of prostate cancer metastatic colonization, we used retroviral RNAi constructs to silence α3 or α6, individually or in combination, in GS689.Li cells, an aggressive, in vivo-passaged subline of PC-3 prostate carcinoma cells [22]. After selection, stably transduced, uncloned populations were FACS-sorted to obtain α3-silenced (GS689.Li-α3si), α6-silenced (GS689.Li-α6si), and α3/α6 doubly silenced (GS689.Li-α3/α6si) cells. Cell surface labeling and immunoprecipitation confirmed the loss of α3 integrin specifically in α3-silenced cells (Fig. 1A, lanes 2 & 4 versus 1 & 3), and the loss of α6 integrin specifically in α6-silenced cells (Fig. 1A, lanes 7 & 8 versus 5 & 6). In GS689.Li cells α6 integrin pairs predominantly with β4 subunit. A small amount of a lower molecular weight species, potentially the α6P cleavage product of the α6 integrin subunit [38], was also detected (Fig 1A, lanes 5–8). Flow cytometry confirmed that the α3si cells showed an ~93% reduction in α3 expression; the α6si cells showed a ~95% reduction in α6 integrin expression; and the α3/α6si cells

showed a ≥95% reduction for both subunits. The expression of another integrin, α2β1, was not dramatically altered in the α3 or α6-silenced cells (Fig. 1A, lanes 9–12).

We next assessed how loss of α3 or α6 integrin affected cell adhesion to their mutual ligand, LM-332. The α3-silenced cells displayed significantly impaired adhesion on LM-332, while the loss of α6 integrin caused a modest reduction in adhesion that was not statistically significant (Fig. 1B). Adhesion on LM-332 was nearly abolished in cells silenced for both α3 and α6. In contrast, all four cell types displayed robust adhesion on the α2β1 integrin ligand, collagen I (Fig. 1B). Collectively, these data established that silencing of α3 integrin led to loss of cell adhesion on LM-332. Integrin α6 may also contribute somewhat to initial adhesion on LM-332, but this contribution is most readily apparent when α3 integrin expression has also been depleted.

Divergent roles of α3 and α6 integrin in metastatic colonization of prostate carcinoma cells

To determine how α3 and α6 integrin may contribute to metastatic colonization, we inoculated GS689.Li wild type (WT), α3si, α6si, and α3/α6si cells into the tail veins of SCID mice (8 mice/cell type). Luciferase expression, present in the wild type parental cells and each of the derived sublines, enabled us to monitor inoculation success and subsequent colonization using bioluminescence imaging (BLI). Immediately after inoculation, BLI confirmed the presence of tumor cells in the lungs of each mouse (Fig. 2A), and tumor burden was then monitored by BLI at weekly intervals. After 5 weeks, the apparent tumor burden caused by α3si cells appeared much greater than that caused by wild type cells, but the tumor burden caused α6si cells was significantly less than wild type (Fig. 2A). Interestingly, growth of the doubly silenced α3/α6si cells was significantly greater than that of the wild type cells, and resembled that of the cells silenced for α3 integrin alone.

BLI quantification over the entire 12 week experiment confirmed that the apparent tumor burden in mice inoculated with α3si or α3/α6si cells became significantly greater than the burden in mice inoculated with wild type cells, beginning on week 4 and continuing for the remainder of the experiment (Fig. 2B). In contrast, tumor growth by α6si cells was delayed and significantly less than wild type cells on week 5. Thereafter, growth of α6si cells increased, and, although the tumor burden in mice with α6si cells remained consistently lower than in mice with wild type cells, the difference was not statistically significant at most time points. However, Kaplan-Meier analysis revealed that survival to endpoint was significantly longer in mice inoculated with α6si cells than in mice inoculated with wild type cells (Fig. 2C). In addition, in contrast to the other three cell types, no extra-thoracic colonization was observed for α6si cells (Fig. 2D), suggesting an impaired ability to disseminate beyond the lungs after tail vein inoculation. In contrast to mice harboring the α6si cells, the survival time of mice inoculated with α3si or α3/α6si cells was significantly less than that of wild type mice (Fig. 2C). Flow cytometric analysis of cells recovered from several independent tumors confirmed that α3 and α6 silencing was maintained in vivo for the duration of the experiment (greater than or equal to 95% silencing for each integrin subunit, data not shown). Thus, α3 and α6 appear to have divergent functions in this model of prostate cancer metastatic colonization, with α3 acting as a suppressor and α6 acting as a promoter. In cells doubly silenced for α3 and α6, the α3 loss-of-function phenotype predominates.

α3-silenced tumor cells display enhanced growth response to stromal cells in 3D co-cultures

Because of the dramatic phenotype of α3-silenced GS689.Li cells in vivo, we next focused on gaining insight into the basis of α3 integrin's apparent metastasis suppressing function in these cells. Cell spreading assays on LM-332 confirmed that the ability of α3si cells to

respond to LM-332 was dramatically impaired (Fig. 3). In proliferation assays, parental and α3si cells displayed similar, modest growth in the absence of serum or exogenous extracellular matrix proteins (Fig. 4A). Plating the cells on LM-332 strongly promoted the ability of the parental cells to grow in serum-free conditions, and this response was partially impaired in the α3si cells (Fig. 4B). The α3si cells also showed modestly impaired growth on collagen I (Fig. 4C). Together with the data in Fig. 1, these data suggested that α3 integrin's ability to promote LM-332-dependent adhesion, spreading, or proliferation may not control GS689.Li cell colonization in vivo, since, in contrast to their impaired performance in these in vitro assays, α3-silenced cells displayed dramatically enhanced metastatic colonization in vivo.

To further explore the basis of the enhanced colonization of the α3-silenced GS689.Li cells, we next assessed the growth of our GS689.Li cell lines in various 3-dimensional (3D) culture settings. When cultured in 3D Matrigel the α3si cells displayed impaired growth compared to the parental cells, in contrast to our in vivo results (Supplementary Fig. 1). Since 3D Matrigel cultures failed to recapitulate in vivo tumor cell responses, we examined alternative 3D culture systems. Tumor cells embedded in or cultured on 3D collagen I in serum-free medium grew poorly, regardless of α3 integrin expression status (not shown; see also Fig. 5G). In contrast, when we cultured GS689.Li cells in serum-free media on top of a 3D collagen I matrix in which MRC-5 human lung fibroblasts were embedded, we observed the selective expansion of the α3si cells (Fig. 5 A–C), similar to our in vivo results. This effect was dose-dependent, as a 3.3 fold increase in the number of fibroblasts in the co-culture nearly doubled the growth of the α3si cells, while having a nominal effect on the growth of the parental tumor cells (Fig. 5D).

To confirm the specificity of the effects of silencing α3 integrin, we developed a second, stably silenced population using an independent α3 targeting shRNA (GS689.Li-α3si-2 cells). Flow cytometry indicated α3si-2 cells retained ~40% of the parental α3 expression level, as compared to the ~7% expression level retained by α3si cells. However, the α3si-2 cells still outgrew the parental cells in the co-culture assay, albeit to a lesser extent than the original α3si cells (Fig. 5E). Thus, silencing α3 expression with two independent constructs yielded tumor cells that responded with enhanced growth in our co-culture assay. Further control experiments confirmed that the vector used to silence α3 expression did not by itself alter α3 function in in vitro assays and had minimal impact on the growth of GS689.Li cells in vitro or in vivo (Supplementary Fig. 2).

To test how our α3-silenced cells would respond to a second relevant stromal cell type, we replaced the MRC-5 fibroblasts with MC3T3-E1 pre-osteoblast-likc cells in our co-culture assay. As shown in Fig. 5F, MC3T3-E1 cells also selectively promoted the growth of the α3si cells. We next examined whether functional blockade of α3 integrin in the parental GS689.Li cells could recapitulate the effects of silencing α3 by RNAi. Antibody blockade of α3 integrin on parental cells significantly promoted their growth compared to untreated controls, to an extent that approached the effect of silencing α3 outright (Fig. 5G). To explore the role of α3 integrin in a second model of aggressive prostate cancer, we assessed α3 integrin expression in the castrate-resistant LNCaP C4-2B cell line. Flow cytometry revealed that C4-2B cells expressed very little α3 integrin (mean fluorescence intensity of 6.3 compared to 3.2 for negative control IgG). We therefore transduced the C4-2B cells with an α3 integrin expression vector to create C4-2B-α3 cells. Flow cytometry confirmed increased α3 expression in C4-2B-α3 cells (mean fluorescence intensity of 52, a value that corresponds to ~60% of the level of α3 expression in GS689.Li parental cells). In our 3D collagen assay, C4-2B-α3 cells and empty vector control cells both showed enhanced growth in the presence of MRC-5 lung fibroblasts. However, the growth of C4-2B-α3 cells was significantly reduced compared to the control cells (Fig. 5G). Thus, in this second cell

system, α3 integrin also appears to exert a growth inhibitory influence in co-cultures with stromal cells. Collectively, these data show that α3 integrin can suppress tumor cell growth in response to stromal cells in a variety of different settings.

MRC-5 fibroblasts secrete one or more heparin-binding factors that selectively promote the growth of α3-silenced tumor cells

Stromal cells might promote tumor cell growth via cell-cell contact or by secreting one or more soluble factors. To begin to explore the mechanism by which stromal cells promote the growth of α3-silenced prostate cancer cells, we examined tumor cell growth on 3D collagen in the presence of different dilutions of MRC-5 fibroblast conditioned medium. Compared to parental cells, which showed a minimal response, the α3-silenced GS689.Li cells displayed a robust, dose-dependent growth response to MRC-5 conditioned medium (Fig. 6A). Since many growth promoting soluble factors bind to heparin, we next fractionated MRC-5 conditioned medium on heparin sepharose prior to use in tumor cell growth assays on 3D collagen. Compared to the starting material, the heparin sepharose flow-through fraction showed significantly reduced growth-promoting activity, suggesting that one or more heparin binding growth factors had been depleted from the conditioned medium by passage over the heparin column (Fig. 6B). Subsequent salt elution steps revealed that one or more heparin-binding growth factors could be eluted from the column, with the greatest activity in the 1M NaCl fraction (Fig. 6B). For all fractions that promoted tumor cell growth, the response of the α3-silenced cells was substantially greater than that of the parental cells.

Discussion

The loss-of-function phenotypes for α3 and α6 integrins in prostate cancer had not previously been described in vivo. Here we show that profound (>90%) silencing of α3 and α6 integrin subunits produced divergent phenotypes in a metastatic colonization assay. Apart from bone, lung is one of the next most frequent sites of prostate cancer metastasis, with lung metastases found in up to 50% of patients who have died with advanced disease [39,40]. Depletion of α6 integrin delayed progressive lung colonization, reduced extra-thoracic dissemination, and enhanced survival, whereas depletion of α3 integrin enhanced colonization and reduced survival time. Since α3 and α6 integrin could potentially compete for ligand binding, it is conceivable that loss of α3 integrin could enhance ligand occupancy of α6 integrins, thereby enabling pro-metastatic α6 integrin functions. However, increased α6 integrin function alone appears unlikely to account for the enhanced colonization of α3-silenced cells, because cells depleted for both α3 and α6 showed enhanced colonization similar to that of cells depleted for only α3 integrin. Interestingly, genetic ablation of tetraspanin CD151, which associates with both α3 and α6 integrins, suppresses spontaneous metastasis in the TRAMP prostate cancer model [41]. It will be important to determine if CD151's pro-metastatic functions in the TRAMP model are exerted through α3 integrin, α6 integrin, or both. PC-3 prostate carcinoma, from which our GS689.Li cells are derived, is an androgen receptor (AR)-negative, PTEN-deficient tumor cell type, and Lamb et al have shown that re-expressing AR in PC-3 cells confers α6β1 integrin-dependent resistance to cell killing by PI 3-kinase inhibitors [25]. Together with Lamb et al, our new data suggests that promoting α3 integrin suppressor functions or blocking α6 integrin promoter functions might represent important therapeutic directions for AR-defective, PTEN-defective prostate cancer.

Several recent studies from Cress and colleagues have implicated α6 integrin in promoting metastatic spread, growth, and invasive behavior of prostate cancer cells, by a mechanism that involves a urokinase plasminogen activator (uPA)-mediated cleavage of the α6 integrin ectodomain [5,29,30,31,42,43]. Analysis of clinical specimens in numerous reports has also implicated α6 integrin in prostate cancer progression (reviewed in [2,3,5,44]). In contrast to

α6 integrin, which has been consistently linked to prostate cancer progression, the role of α3 integrin is less clear. In one early study, in vitro selection of PC-3 prostate carcinoma cells for enhanced Matrigel invasion yielded a sub-population with reduced α3 integrin expression [32]. These α3-low expressers were reported to display enhanced colonization in vivo as well [32]. Examination of α3 and α6 integrin expression profiles in clinical prostate cancer samples revealed different classes with different combinations of integrin subunit expression [8]. This study suggested that in higher pathological stages, there may be a selection for α6 integrin expression, and against a class of tumors in which α3 is the only laminin-binding integrin expressed. On the other hand, in early stages of prostate carcinoma invasion, neoplastic cells could potentially use α3β1 integrin to adhere and invade through the remnants of the LM-332-rich basement membrane that was deposited by basal prostate epithelial cells [45], or for collective migration on LM-511, which is retained in invasive prostate cancer [44]. Conflicting data for α3 integrin have been also been reported in several other types of cancer [33]; however little loss-of-function data has been available until recently. Mitchell et al recently showed that silencing α3 integrin in MDA-MB-231 breast carcinoma cells impaired tumor growth after subcutaneous or orthotopic fat pad implantation [46]. In this study, reduced cyclooxygenase-2 (COX-2) expression occurred concurrently with α3 integrin silencing, resulting in reduced production of prostaglandin E2 (PGE2) and reduced PGE2-dependent tumor cell invasion and cross-talk to endothelial cells [46].

Our study reveals that in contrast to the results from the aforementioned breast carcinoma model, loss of α3 expression can promote a more metastatic phenotype in a prostate carcinoma model. Common to both Mitchell et al and our study are results that suggest that loss of α3 integrin can dramatically influence tumor-host interactions. While loss of α3 in MDA-MB-231 cells reduced the ability of tumor cells to secrete a factor that promotes endothelial cell migration [46], in GS689.Li prostate cancer cells, loss of α3 appeared to enhance the ability of the tumor cells to respond to one or more heparin binding growth factors secreted by stromal cells. One appealing candidate factor is hepatocyte growth factor (HGF), given that its receptor is highly expressed by PC-3 cells and can be transactivated by PC-3 cell adhesion on integrin ligands [47]. However, function blocking anti-HGF antibodies failed to influence growth in our 3D co-culture assay (Varzavand and Stipp, unpublished observation). Studies to identify the factors produced by stromal cells that elicit α3 integrin-dependent tumor cell responses are an important future direction. It will also be important to determine the range of different tumor-host responses that are influenced by tumoral α3 integrin expression. Interestingly, loss of α3 expression in endothelial cells enhances pathological angiogenesis and tumor growth by upregulating endothelial cell responsiveness to vascular endothelial growth factor signaling [48]. In addition, genetic deletion of α3 integrin specifically in keratinocytes impaired the ability of the keratinocytes to respond to stromal TGFβ during wound healing [49]. Thus, regulating cell responses to autocrine and juxtracrine signaling appears to be an emerging theme for α3 integrin function. Lastly, our data also raise the possibility that α3β1 integrin promotes tumor growth at primary sites, such as the mammary fat pad in Mitchell et al, but can play an opposite role in later colonization events.

In conclusion, our data reveal that α3 integrin can act as a suppressor of metastatic growth by a mechanism that may involve limiting tumor cell response to stromal-derived growth factors. These new data provide an important counterexample to studies implicating α3 integrin as a promoter of metastasis. Our new system should prove useful for exploring this important, contrasting function of α3 integrin in cancer.

Supplementary Material

Refer to Web version on PubMed Central for supplementary material.

Acknowledgments

We thank the University of Iowa Flow Cytometry Core Facility for assistance with cell sorting. This work was supported by NIH R01 CA136664, American Cancer Society RSG-07-043-01-CSM, and DOD W81XWH-07-1-0043 (C. S. S.), NIH R01 CA130916 (M. D. H.) and American Heart Association Predoctoral Fellowship 0610074Z (J. M. D.)

References

1. Siegel R, Naishadham D, Jemal A. Cancer statistics, 2012. CA Cancer J Clin. 2012; 62:10–29. [PubMed: 22237781]
2. Goel HL, Alam N, Johnson INS, Languino LR. Integrin signaling aberrations in prostate cancer. Am J Transl Res. 2009; 1:211–220. [PubMed: 19956432]
3. Goel HL, Li J, Kogan S, Languino LR. Integrins in prostate cancer progression. Endocr Relat Cancer. 2008; 15:657–664. [PubMed: 18524948]
4. Knudsen BS, Miranti CK. The impact of cell adhesion changes on proliferation and survival during prostate cancer development and progression. J Cell Biochem. 2006; 99:345–361. [PubMed: 16676354]
5. Sroka IC, Anderson TA, McDaniel KM, Nagle RB, Gretzer MB, et al. The laminin binding integrin alpha6beta1 in prostate cancer perineural invasion. J Cell Physiol. 2010; 224:283–288. [PubMed: 20432448]
6. Davis TL, Cress AE, Dalkin BL, Nagle RB. Unique expression pattern of the alpha6beta4 integrin and laminin-5 in human prostate carcinoma. Prostate. 2001; 46:240–248. [PubMed: 11170153]
7. Hao J, Jackson L, Calaluce R, McDaniel K, Dalkin BL, et al. Investigation into the mechanism of the loss of laminin 5 (alpha3beta3gamma2) expression in prostate cancer. Am J Pathol. 2001; 158:1129–1135. [PubMed: 11238061]
8. Schmelz M, Cress AE, Scott KM, Bürger F, Cui H, et al. Different phenotypes in human prostate cancer: alpha6 or alpha3 integrin in cell-extracellular adhesion sites. Neoplasia. 2002; 4:243–254. [PubMed: 11988844]
9. Nishiuchi R, Takagi J, Hayashi M, Ido H, Yagi Y, et al. Ligand-binding specificities of laminin-binding integrins: a comprehensive survey of laminin-integrin interactions using recombinant alpha3beta1, alpha6beta1, alpha7beta1 and alpha6beta4 integrins. Matrix Biol. 2006; 25:189–197. [PubMed: 16413178]
10. Jones JC, Hopkinson SB, Goldfinger LE. Structure and assembly of hemidesmosomes. Bioessays. 1998; 20:488–494. [PubMed: 9699461]
11. Frank DE, Carter WG. Laminin 5 deposition regulates keratinocyte polarization and persistent migration. J Cell Sci. 2004; 117:1351–1363. [PubMed: 14996912]
12. Gu J, Sumida Y, Sanzen N, Sekiguchi K. Laminin-10/11 and fibronectin differentially regulate integrin-dependent Rho and Rac activation via p130(Cas)-CrkII-DOCK180 pathway. J Biol Chem. 2001; 276:27090–27097. [PubMed: 11369773]
13. Winterwood NE, Varzavand A, Meland MN, Ashman LK, Stipp CS. A critical role for tetraspanin CD151 in alpha3beta1 and alpha6beta4 integrin-dependent tumor cell functions on laminin-5. Mol Biol Cell. 2006; 17:2707–2721. [PubMed: 16571677]
14. Zhou H, Kramer RH. Integrin engagement differentially modulates epithelial cell motility by RhoA/ROCK and PAK1. J Biol Chem. 2005; 280:10624–10635. [PubMed: 15611088]
15. Chattopadhyay N, Wang Z, Ashman LK, Brady-Kalnay SM, Kreidberg JA. alpha3beta1 integrin-CD151, a component of the cadherin-catenin complex, regulates PTPmu expression and cell-cell adhesion. J Cell Biol. 2003; 163:1351–1362. [PubMed: 14691142]
16. DiPersio CM, Hodivala-Dilke KM, Jaenisch R, Kreidberg JA, Hynes RO. alpha3beta1 Integrin is required for normal development of the epidermal basement membrane. J Cell Biol. 1997; 137:729–742. [PubMed: 9151677]

17. Johnson JL, Winterwood N, DeMali KA, Stipp CS. Tetraspanin CD151 regulates RhoA activation and the dynamic stability of carcinoma cell-cell contacts. J Cell Sci. 2009; 122:2263–2273. [PubMed: 19509057]

18. Kreidberg JA, Donovan MJ, Goldstein SL, Rennke H, Shepherd K, et al. Alpha 3 beta 1 integrin has a crucial role in kidney and lung organogenesis. Development. 1996; 122:3537–3547. [PubMed: 8951069]

19. Allen MV, Smith GJ, Juliano R, Maygarden SJ, Mohler JL. Downregulation of the beta4 integrin subunit in prostatic carcinoma and prostatic intraepithelial neoplasia. Hum Pathol. 1998; 29:311–318. [PubMed: 9563778]

20. Cress AE, Rabinovitz I, Zhu W, Nagle RB. The alpha 6 beta 1 and alpha 6 beta 4 integrins in human prostate cancer progression. Cancer Metastasis Rev. 1995; 14:219–228. [PubMed: 8548870]

21. Nagle RB, Hao J, Knox JD, Dalkin BL, Clark V, et al. Expression of hemidesmosomal and extracellular matrix proteins by normal and malignant human prostate tissue. Am J Pathol. 1995; 146:1498–1507. [PubMed: 7778688]

22. Drake JM, Strohbehn G, Bair TB, Moreland JG, Henry MD. ZEB1 enhances transendothelial migration and represses the epithelial phenotype of prostate cancer cells. Mol Biol Cell. 2009; 20:2207–2217. [PubMed: 19225155]

23. Drake JM, Barnes JM, Madsen JM, Domann FE, Stipp CS, et al. ZEB1 coordinately regulates laminin-332 and {beta}4 integrin expression altering the invasive phenotype of prostate cancer cells. J Biol Chem. 2010; 285:33940–33948. [PubMed: 20729552]

24. Bair EL, Chen ML, McDaniel K, Sekiguchi K, Cress AE, et al. Membrane type 1 matrix metalloprotease cleaves laminin-10 and promotes prostate cancer cell migration. Neoplasia. 2005; 7:380–389. [PubMed: 15967115]

25. Lamb LE, Zarif JC, Miranti CK. The Androgen Receptor Induces Integrin {alpha}6{beta}1 to Promote Prostate Tumor Cell Survival via NF-{kappa}B and Bcl-xL Independently of PI3K Signaling. Cancer Res. 2011

26. Hallmann R, Horn N, Selg M, Wendler O, Pausch F, et al. Expression and function of laminins in the embryonic and mature vasculature. Physiol Rev. 2005; 85:979–1000. [PubMed: 15987800]

27. Gu Y, Sorokin L, Durbeej M, Hjalt T, Jönsson JI, et al. Characterization of bone marrow laminins and identification of alpha5-containing laminins as adhesive proteins for multipotent hematopoietic FDCP-Mix cells. Blood. 1999; 93:2533–2542. [PubMed: 10194432]

28. Siler U, Seiffert M, Puch S, Richards A, Torok-Storb B, et al. Characterization and functional analysis of laminin isoforms in human bone marrow. Blood. 2000; 96:4194–4203. [PubMed: 11110691]

29. Pawar SC, Demetriou MC, Nagle RB, Bowden GT, Cress AE. Integrin alpha6 cleavage: a novel modification to modulate cell migration. Exp Cell Res. 2007; 313:1080–1089. [PubMed: 17303120]

30. King TE, Pawar SC, Majuta L, Sroka IC, Wynn D, et al. The role of alpha 6 integrin in prostate cancer migration and bone pain in a novel xenograft model. PLoS ONE. 2008; 3:e3535. [PubMed: 18958175]

31. Ports MO, Nagle RB, Pond GD, Cress AE. Extracellular engagement of alpha6 integrin inhibited urokinase-type plasminogen activator-mediated cleavage and delayed human prostate bone metastasis. Cancer Research. 2009; 69:5007–5014. [PubMed: 19491258]

32. Dedhar S, Saulnier R, Nagle R, Overall CM. Specific alterations in the expression of alpha 3 beta 1 and alpha 6 beta 4 integrins in highly invasive and metastatic variants of human prostate carcinoma cells selected by in vitro invasion through reconstituted basement membrane. Clin Exp Metastasis. 1993; 11:391–400. [PubMed: 8375114]

33. Stipp CS. Laminin-binding integrins and their tetraspanin partners as potential antimetastatic targets. Expert Rev Mol Med. 2010; 12:e3. [PubMed: 20078909]

34. Bergelson JM, St JN, Kawaguchi S, Pasqualini R, Berdichevsky F, et al. The I domain is essential for echovirus 1 interaction with VLA-2. Cell Adhes Commun. 1994; 2:455–464. [PubMed: 7842258]

35. Weitzman JB, Pasqualini R, Takada Y, Hemler ME. The function and distinctive regulation of the integrin VLA-3 in cell adhesion, spreading, and homotypic cell aggregation. J Biol Chem. 1993; 268:8651–8657. [PubMed: 8473308]
36. Drake JM, Gabriel CL, Henry MD. Assessing tumor growth and distribution in a model of prostate cancer metastasis using bioluminescence imaging. Clin Exp Metastasis. 2005; 22:674–684. [PubMed: 16703413]
37. Rasband, W. ImageJ. Bethesda, Maryland, USA: US National Institutes of Health; (1997–2012). http://imagej.nih.gov/ij/.
38. Demetriou MC, Cress AE. Integrin clipping: a novel adhesion switch? J Cell Biochem. 2004; 91:26–35. [PubMed: 14689578]
39. Bubendorf L, Schöpfer A, Wagner U, Sauter G, Moch H, et al. Metastatic patterns of prostate cancer: an autopsy study of 1,589 patients. Hum Pathol. 2000; 31:578–583. [PubMed: 10836297]
40. Shah RB, Mehra R, Chinnaiyan AM, Shen R, Ghosh D, et al. Androgen-independent prostate cancer is a heterogeneous group of diseases: lessons from a rapid autopsy program. Cancer Res. 2004; 64:9209–9216. [PubMed: 15604294]
41. Copeland BT, Bowman MJ, Ashman LK. Genetic Ablation of the Tetraspanin Cd151 Reduces Spontaneous Metastatic Spread of Prostate Cancer in the TRAMP Model. Mol Cancer Res. 2012
42. Pawar SC, Dougherty S, Pennington ME, Demetriou MC, Stea BD, et al. alpha6 integrin cleavage: sensitizing human prostate cancer to ionizing radiation. Int J Radiat Biol. 2007; 83:761–767. [PubMed: 18058365]
43. Sroka IC, Sandoval CP, Chopra H, Gard JM, Pawar SC, et al. Macrophage-dependent cleavage of the laminin receptor alpha6beta1 in prostate cancer. Mol Cancer Res. 2011; 9:1319–1328. [PubMed: 21824975]
44. Nagle RB, Cress AE. Metastasis Update: Human Prostate Carcinoma Invasion via Tubulogenesis. Prostate Cancer. 2011; 2011 249290.
45. Yu H-M, Frank DE, Zhang J, You X, Carter WG, et al. Basal prostate epithelial cells stimulate the migration of prostate cancer cells. Mol Carcinog. 2004; 41:85–97. [PubMed: 15378647]
46. Mitchell K, Svenson KB, Longmate WM, Gkirtzimanaki K, Sadej R, et al. Suppression of Integrin {alpha}3{beta}1 in Breast Cancer Cells Reduces Cyclooxygenase-2 Gene Expression and Inhibits Tumorigenesis, Invasion, and Cross-Talk to Endothelial Cells. Cancer Research. 2010
47. Sridhar SC, Miranti CK. Tetraspanin KAI1/CD82 suppresses invasion by inhibiting integrin-dependent crosstalk with c-Met receptor and Src kinases. Oncogene. 2006; 25:2367–2378. [PubMed: 16331263]
48. da Silva RG, Tavora B, Robinson SD, Reynolds LE, Szekeres C, et al. Endothelial alpha3beta1-integrin represses pathological angiogenesis and sustains endothelial-VEGF. Am J Pathol. 2010; 177:1534–1548. [PubMed: 20639457]
49. Reynolds LE, Conti FJ, Silva R, Robinson SD, Iyer V, et al. alpha3beta1 integrin-controlled Smad7 regulates reepithelialization during wound healing in mice. J Clin Invest. 2008; 118:965–974. [PubMed: 18246199]

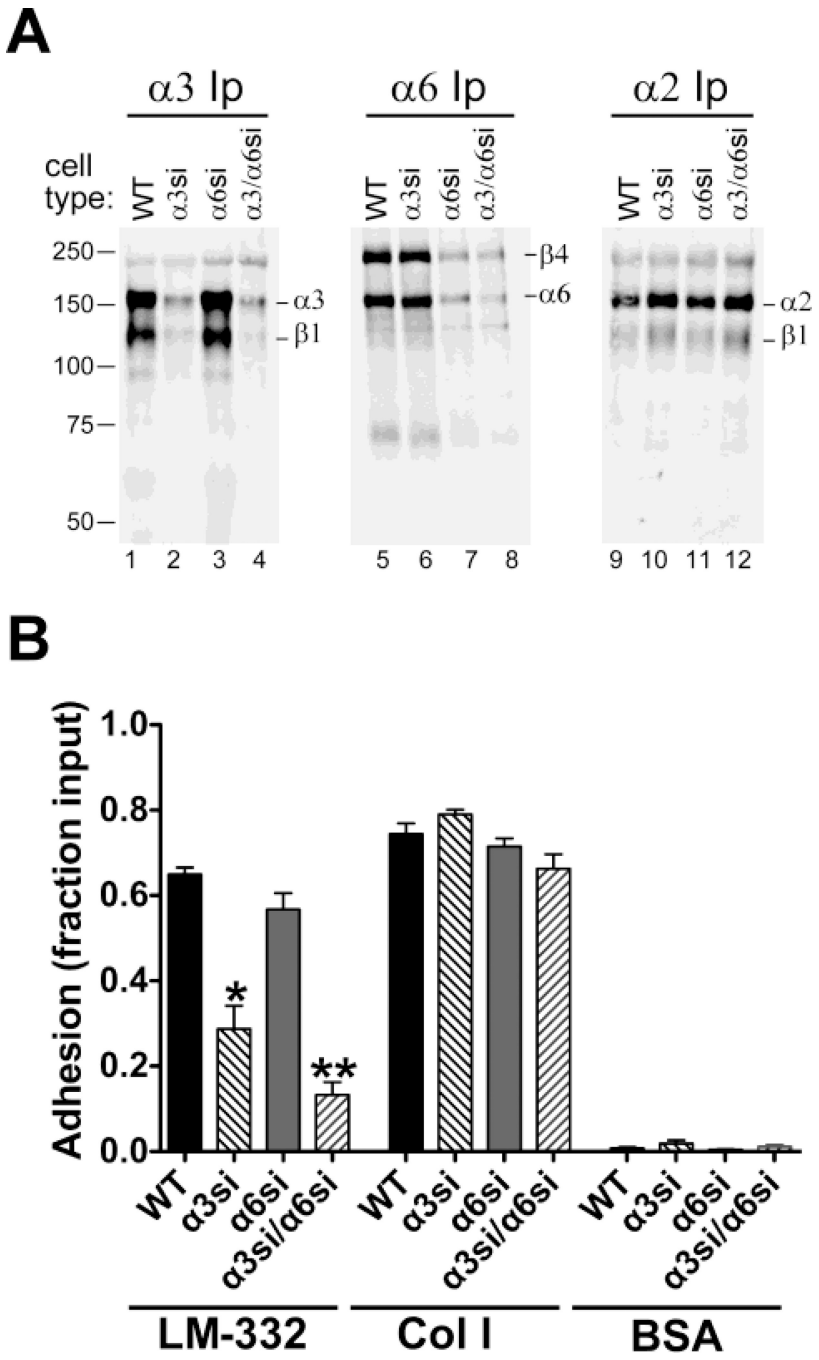

Fig. 1.

Specific silencing of α3 and α6 integrin subunits in GS698.Li prostate carcinoma cells. **a** Parental (*WT*), α3-silenced (α*3si*), α6-silenced (α*6si*), and doubly silenced cells (α*3*/α*6si*) were surface-labeled with biotin and extracted with 1% Triton X-100. Integrins α3β1, α6β4, or α2β1 were immunoprecipitated (*Ip*) from normalized lysates, and then analyzed by blotting with IRdye 800-streptavidin. **b** WT, α3si, α6si, and α3/α6si cells were allowed to adhere to wells coated with laminin-332 (*LM-332*), collagen I (*Col I*), or BSA for 20 min in serum-free medium. Non-adherent cells were removed by rinsing, and adherent cells were fixed and quantified by staining with crystal violet. Results are presented as a fraction of

total cells input, as measured in poly-L-lysine control wells. Two independent trials that gave similar results were pooled (for total of 8 wells per cell type/condition) Error bars indicate S.E.M. *Significantly less than WT parental cells, ANOVA with Tukey-Kramer t test, ($p<0.001$); **Significantly less than WT ($p<0.001$) and significantly less than α3si ($p<0.05$), ANOVA with Tukey-Kramer t test.

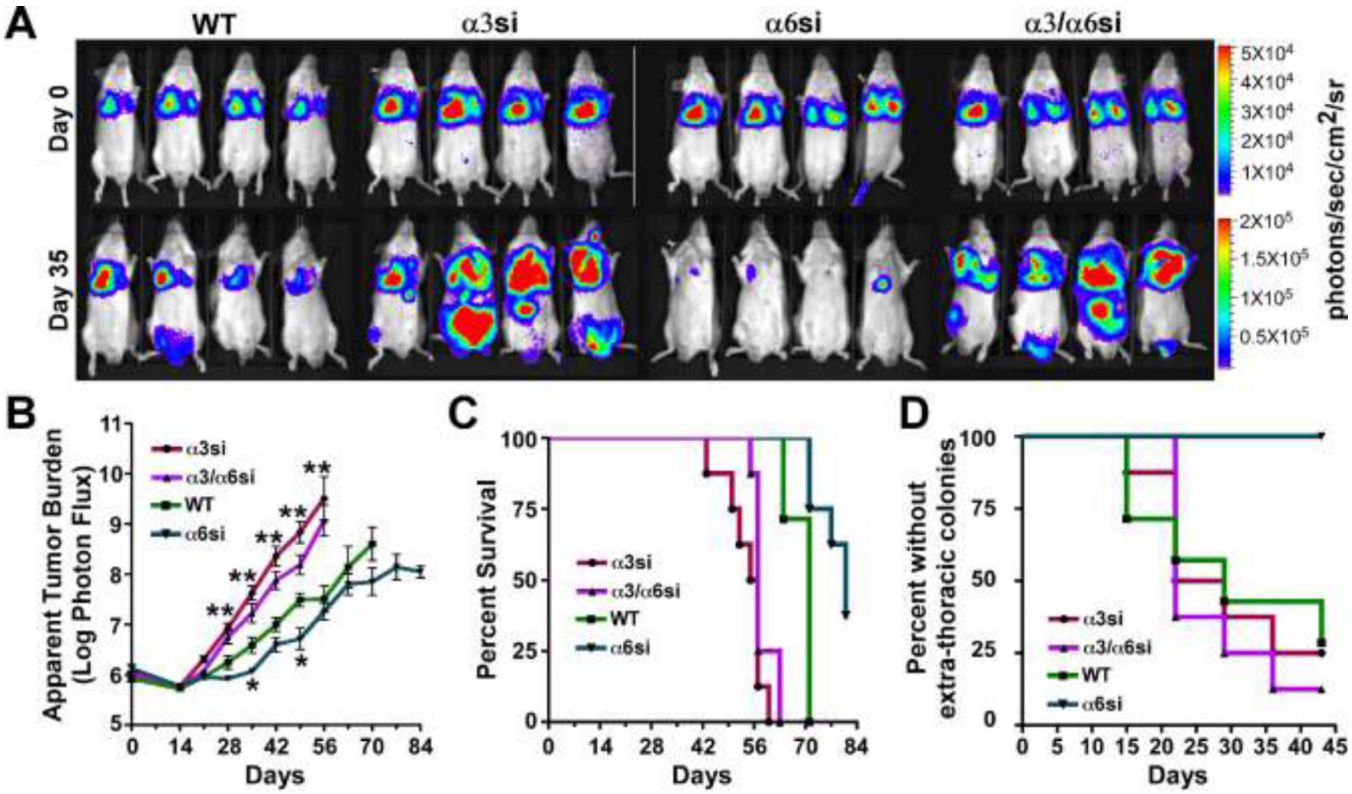

Fig. 2.

Divergent functions for α3 and α6 integrins in metastatic colonization of GS689.Li prostate carcinoma cells. **a** Bioluminescence imaging (BLI) was used to visualize WT, α3si, α6si, and α3/α6si GS689.Li cells immediately after tail vein inoculation (Day 0) or 35 days later. Eight mice per cell type were injected, four of each group are depicted. Note that the photon flux color scale is 4 fold higher on week 5 than on day 0. **b** The average apparent tumor burden for each group was measured each week by BLI, as described in Materials and Methods. Statistical analysis: significantly different from WT parental cells, ANOVA with Dunnett t test (*$p<0.05$, **$p<0.01$ or lower). **c** Kaplan-Meier analysis of the percent survival to endpoint for the 8 mice per group (using criteria described in Materials and Methods) revealed significantly reduced survival times for α3si and α3/α6si cells ($p<0.0002$) and significantly increased survival time for α6si cells ($p<0.003$) as compared to WT parental cells. **d** Kaplan-Meier analysis of extra-thoracic colonization revealed significantly reduced colonization for α6si cells compared to the other groups ($p<0.004$).

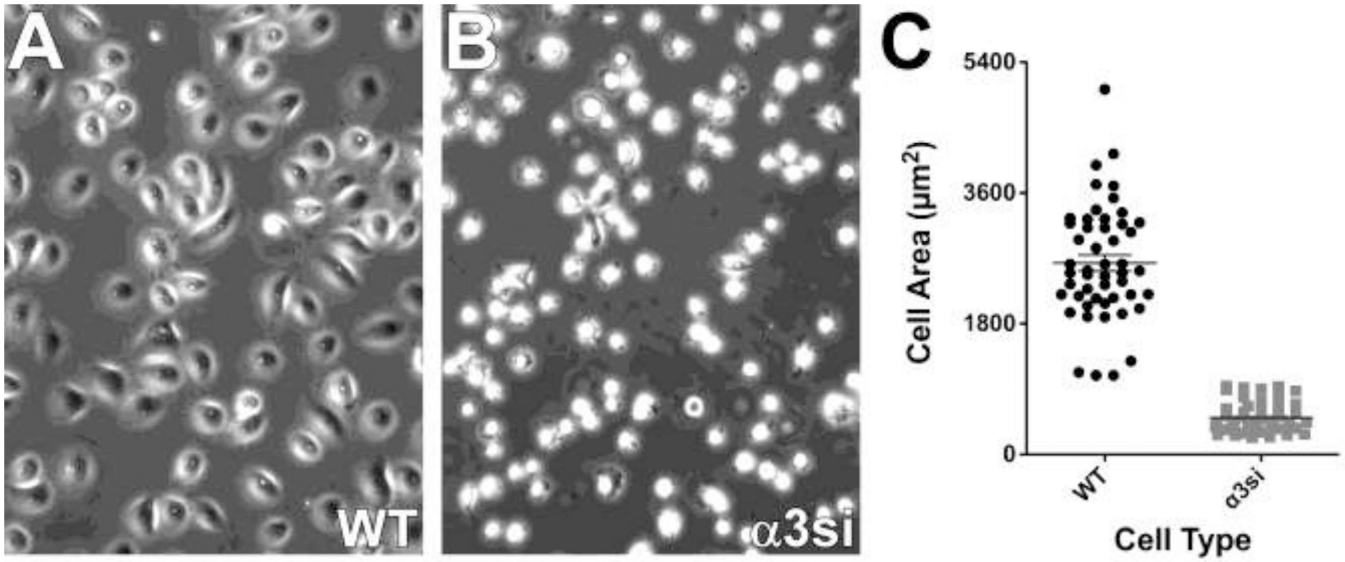

Fig. 3.

Severely impaired spreading of α3 silenced cells on LM-332. **a & b** WT and α3si cells were plated in serum-free medium on LM-332-coated glass bottom culture dishes. After 30 min for cell attachment and spreading, cells were photographed with a 20X objective. **c** 50 cells of each type were quantified using ImageJ to measure cell area. The α3si cells were significantly less well spread, $p < 0.0001$, unpaired t test.

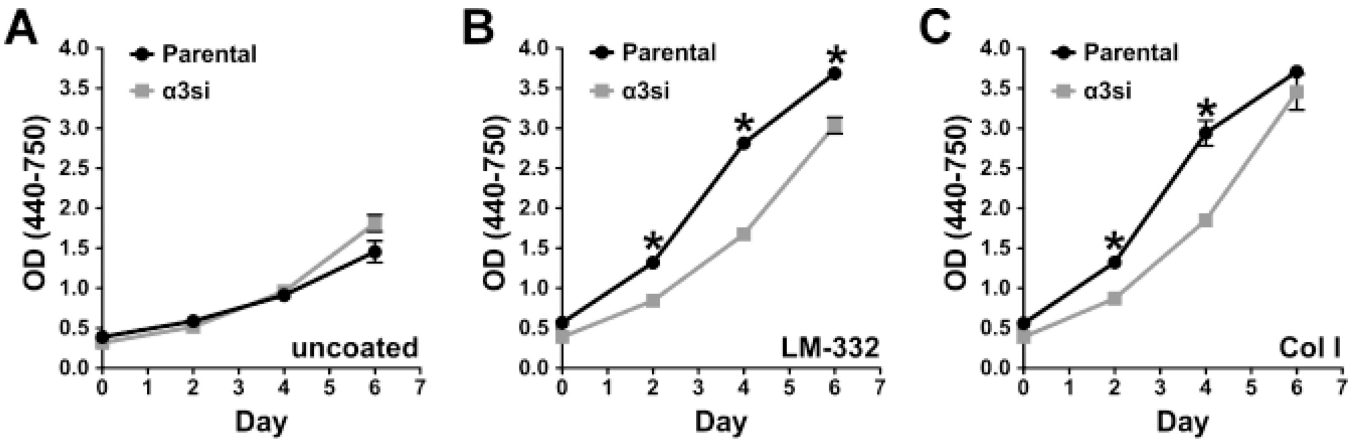

Fig. 4.

Analysis of in vitro GS689.Li tumor cell proliferation. WT and α3si cells were plated in serum-free medium in 96 well plates in (**a**) uncoated wells, (**b**) laminin-332-coated wells, or (**c**) collagen I-coated wells. Replicate plates were analyzed on successive days by a WST colorimetric assay (6 wells/cell type per time point). Statistical analysis: *value for WT cells was significantly higher than that of α3si cells ($p<0.001$, unpaired t test).

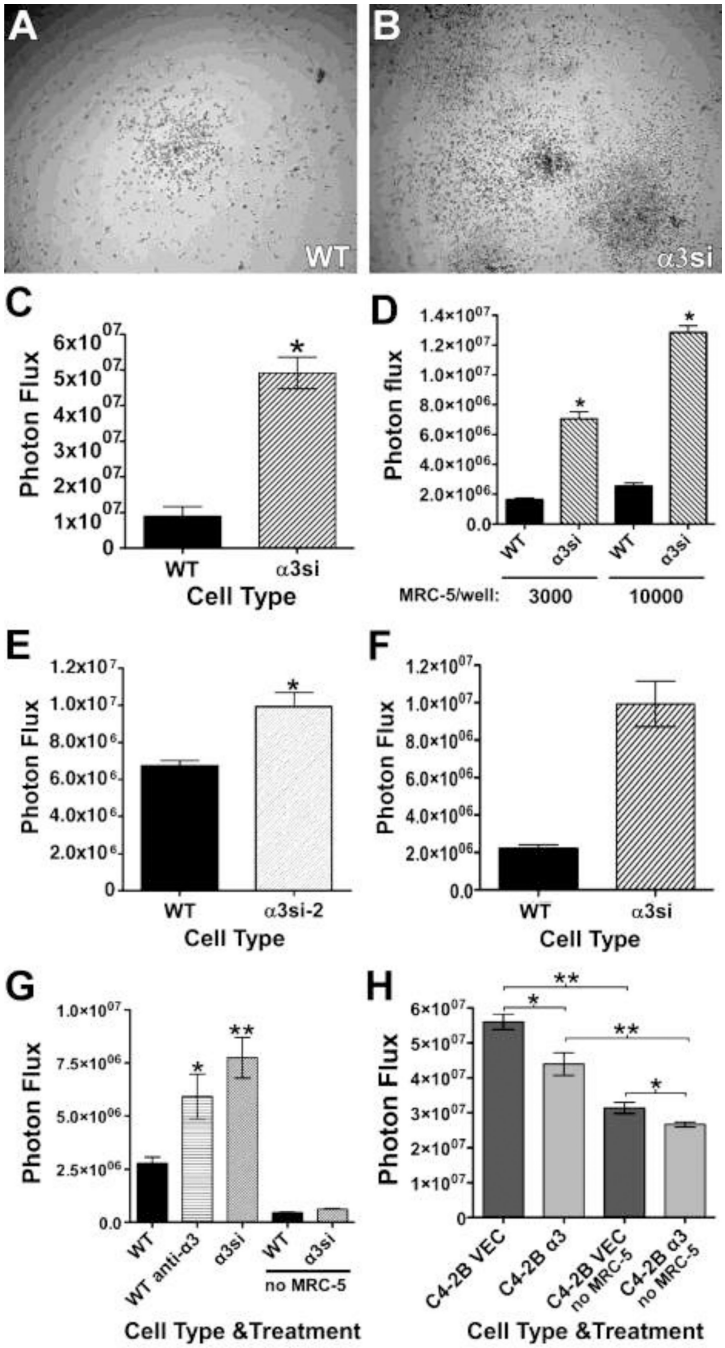

Fig. 5.

α3 integrin negatively regulates tumor cell growth in 3D co-cultures with stromal cells. **a & b** WT or α3si GS689.Li cells (3,000 cells per well) were plated on 3D collagen in which 10,000 MRC-5 human lung fibroblasts per well had been embedded. After 17 d, cells were photographed with a 4X objective. **c** A co-culture experiment was performed as described in a & b, and tumor cell number was quantified using bioluminescence imaging (BLI) after 28 d. *Significantly greater than WT, $p<0.0001$, unpaired t test, (n=5 wells/cell type). **d** WT or α3si tumor cells (3,000/well) were plated on 3D collagen in which 3,000 or 10,000 MRC-5 human lung fibroblasts per well had been embedded. After 24 d, tumor cell number was

quantified by BLI. *Significantly greater than WT, p<0.0001, unpaired t test (n=6 wells/cell type). **e** A co-culture experiment was performed as described in a & b, but comparing WT to α3si-2 cells, in which residual cell surface α3 is ~40% of WT α3 expression. After 28 d, tumor cell number was quantified by BLI. *Significantly greater than WT, p<0.001, unpaired t test, (n=10 wells/cell type). **f** A co-culture experiment was performed as in a & b, except that 10,000 MC3T3-E1 pre-osteoblast-like cells per well were embedded in collagen instead of 10,000 MRC-5 fibroblasts. After 18 d, tumor cell number was quantified by BLI. *Significantly greater than WT, p<0.0001, unpaired t test (n=6 wells/cell type). **g** A co-culture experiment was performed as in a & b, but comparing untreated WT tumor cells (*WT*), WT tumor cells treated with 10 μg/ml A3-IIF5 anti-α3 integrin antibody (*WT anti-α3*), and α3si tumor cells (*α3si*). In addition, MRC-5 cells were omitted from one set each of WT and α3si wells (*no MRC-5*). After 16 d, tumor cell number was quantified by BLI. Statistical analysis: significantly greater than untreated WT wells, *p<0.05, **p<0.01, ANOVA with Tukey-Kramer t test (n=6 wells/cell type). **h** LNCaP C4-2B prostate carcinoma cells transduced with empty vector (*C4-2B VEC*) or with an α3 integrin expression vector (*C4-2B α3*) were plated at 3,000 cells per well on (i) 3D collagen in which 10,000 MRC-5 fibroblasts per well had been embedded, or (ii) on 3D collagen lacking MRC-5 cells (*no MRC-5*). After 26 d, tumor cell number was quantified by BLI. Statistical analysis: the indicated comparisons were significant at *p<0.01, **p<0.001, ANOVA with Tukey-Kramer t test (n=6 wells/cell type); Graphs in C-H all depict mean ± S.E.M.

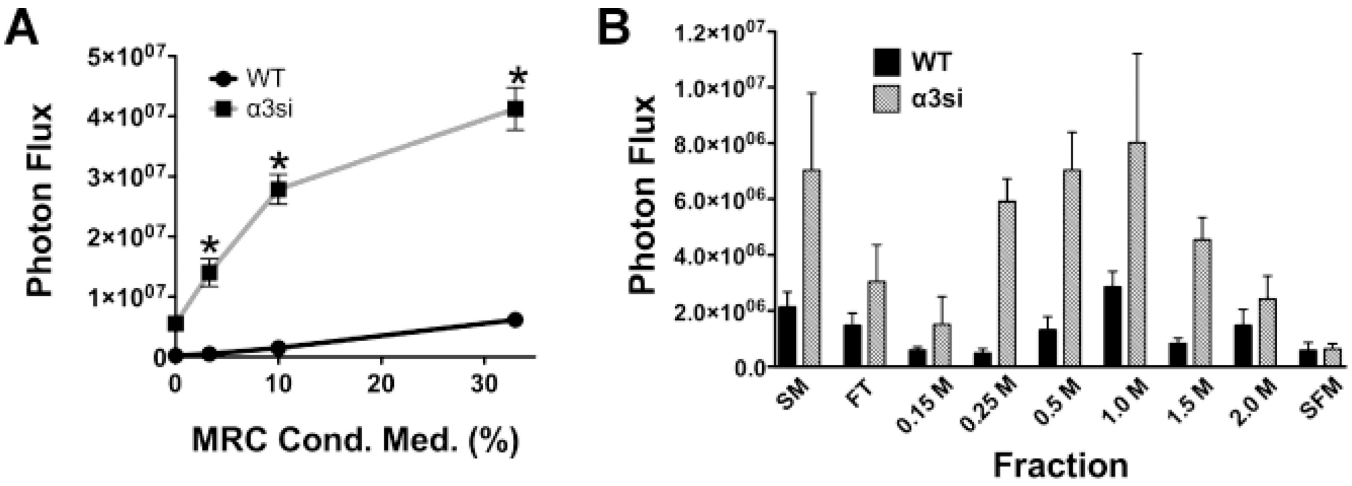

Fig. 6.

MRC-5 fibroblasts secrete one or more heparin-binding factors that selectively promote the growth of α3-silenced GS689.Li tumor cells. Freshly confluent cultures of MRC-5 fibroblasts were used to condition serum-free medium for 3 days, and then the medium was harvested and used in tumor cell growth assays. **a** WT and α3si GS689.Li tumor cells (3,000 cells/well) were plated on 3D collagen in varying dilutions of MRC-5 conditioned medium ranging from 0% (non-conditioned medium) to 33% (MRC-5 conditioned medium diluted 1:3 in non-conditioned medium). Wells were refed after 1 wk with fresh dilutions of MRC-5 conditioned medium. After 2 wks, tumor cell number was quantified by bioluminescence imaging (BLI). The α3si cells displayed a dramatically enhanced dose-response to MRC-5 conditioned medium. *Significantly greater than WT wells, $p<0.0001$, unpaired t test (n=4 wells/cell type). Values plotted are mean ± S.E.M. **b** MRC-5 conditioned medium was fractionated on heparin sepharose, as described in Materials and Methods. Fractions were diluted 1:8 and then used in growth assays of WT and α3si tumor cells on 3D collagen as in panel a. *SM*, starting material; *FT*, flow through; *0.15 M – 2.0M*, NaCl elution steps of the heparin sepharose column, *SFM*, non-conditioned, serum-free medium. Values plotted are mean ± S.E.M. for 3 wells/cell type/condition.